



University  
of Glasgow

Sun, Q.-J., Zhao, X.-H., Yeung, C.-C., Tian, Q., Kong, K.-W., Wu, W., Venkatesh, S., Li, W.-J. and Roy, V. A.L. (2020) Bioinspired, self-powered, and highly sensitive electronic skin for sensing static and dynamic pressures. *ACS Applied Materials and Interfaces*, 12(33), pp. 37239-37247.

(doi: [10.1021/acsami.0c10788](https://doi.org/10.1021/acsami.0c10788))

This is the Author Accepted Manuscript.

There may be differences between this version and the published version. You are advised to consult the publisher's version if you wish to cite from it.

<https://eprints.gla.ac.uk/221479/>

Deposited on: 27 July 2020

# Bio-Inspired, Self-Powered, Highly Sensitive Electronic Skin for Sensing Static and Dynamic Pressures

*Qi-Jun Sun<sup>a‡</sup>, Xin-Hua Zhao<sup>b‡</sup>, Chi-Chung Yeung<sup>c</sup>, Qiong Tian<sup>a</sup>, Ka-Wai Kong<sup>d</sup>, Wei Wu<sup>a</sup>,  
Shishir Venkatesh<sup>a</sup>, Wen-Jung Li<sup>d</sup>, and Vellaisamy A. L. Roy<sup>a\*</sup>*

<sup>a</sup>State Key Laboratory of Terahertz and Millimeter Waves and Department of Materials Science & Engineering, City University of Hong Kong, Kowloon, Hong Kong 999077, China.

<sup>b</sup>Department of Chemistry, Southern University of Science and Technology, Shenzhen 518055, China.

<sup>c</sup>Department of Chemistry, City University of Hong Kong, Kowloon, Hong Kong 999077, China.

<sup>d</sup>Department of Mechanical Engineering, City University of Hong Kong, Kowloon, Hong Kong 999077, China.

## **KEYWORDS**

Self-powered, Bio-inspired, Redox-induced electricity, Electronic skin, Health monitoring

## **ABSTRACT**

Flexible piezoresistive pressure sensors obtain global research interest owing to their potential applications in healthcare, human-robotic interaction, and artificial nerves. However, an additional power supply is usually required to drive the sensors, which results in increased complexity of the pressure sensing system. Despite the great efforts in pursuing self-powered pressure sensors, most of the self-powered devices can merely detect the dynamic pressure and the reliable static pressure detection is still challenging. With the help of redox-induced

electricity, a bio-inspired graphite/polydimethylsiloxane piezoresistive composite film acting both as the cathode and pressure sensing layer, a neoteric electronic skin sensor is presented here to detect not only the dynamic forces but also the static forces without external power supply. Additionally, the sensor exhibits a fascinating pressure sensitivity of  $\sim 10^3 \text{ kPa}^{-1}$  over a broad sensing range from 0.02 to 30 kPa. Benefiting from the advanced performance of the device, various potential applications including arterial pulse monitoring, human motion detecting, and Morse code generation are successfully demonstrated. This new strategy could pave a way for the development of next-generation self-powered wearable devices.

## INTRODUCTION

Wearable and flexible electronics, especially the self-powered sensors, are attracting unprecedented research interest due to their potential application in wearables. Among them, pressure sensors have potential applications in health monitoring,<sup>1-9</sup> human-machine interaction,<sup>11-14</sup> prosthetics,<sup>15,16</sup> and bio-inspired artificial nerves.<sup>17,18</sup> Based on various sensing mechanisms, different types of prevalent pressure sensing devices: capacitive,<sup>19-23</sup> piezoresistive,<sup>24-27</sup> piezoelectric,<sup>28-30</sup> and triboelectric sensors<sup>31-41</sup> have been reported. Pressure sensors based on capacitive and piezoresistive structures can detect both dynamic and static pressures, however, a power supply is essential for these sensors.<sup>42-46</sup> On the other hand, piezoelectric and triboelectric sensors can be self-powered in measuring dynamic pressures but reliable static pressure detection is of great challenge.<sup>47,48</sup> Therefore, it is still challenging to achieve self-powered pressure sensors for reliable detection of dynamic and static pressure simultaneously.

Generally, piezoresistive pressure sensors have attracted much more attentions than the other types due to the easier fabrication procedures and less stringent electrical configurations. Currently, tremendous efforts have been paid by the researchers in pursuing a high sensitivity and/or a broad pressure sensing range for piezoresistive pressure sensors but little attention has been paid in achieving self-powered piezoresistive devices.<sup>3,11,12,49</sup> Recently, He et al. reported a flexible pressure sensor device with a high sensitivity of  $1875.53 \text{ kPa}^{-1}$  over a broad detection range of 0-40 kPa by developing an innovative material construction strategy to obtain a self-assembled graphene active layer, in which the thickness and conductivity of the sensing film could be well balanced.<sup>50</sup> However, despite the fascinating achievement in pressure sensitivity and sensing range, the fabrication procedure of the tactile sensor is complicated and a power supply is required. Pyo and co-workers demonstrated a tactile sensor based on hierarchically structured fabric with multi-layers by developing a simple and inexpensive fabrication strategy. The sensor exhibited excellent device properties including a

sensitivity of  $26.13 \text{ kPa}^{-1}$ , a wide pressure range of 0.2-982 kPa, and a fast response as well.<sup>11</sup> Although cost-effective fabric was used to obtain tactile sensors with intriguing sensitivity over broad pressure sensing range for dynamic and static pressure detection, an additional power supply is required to drive the sensor. It is not energy-efficient and may increase the complexity of the pressure sensing system as well. For the ideal future flexible pressure sensors with self-powered capability are highly desired. Recently, nanogenerators, converting the mechanical energy into electrical power via a coupling of triboelectrification and electrostatic induction, have attracted extensive attentions for their potential applications in self-powered sensors and electronic systems.<sup>31,34,41</sup> Although the triboelectric nanogenerators can detect the static pressure by measuring output voltage theoretically, undesired signal decay usually occurs.<sup>47,48</sup> Therefore, nanogenerators are mostly used to detect the dynamic pressure instead of the static pressure. However, reliable static pressure detection is crucial for various potential applications such as planar foot pressure distribution mapping, health monitoring, electronic skin (e-skin), etc. Therefore, issues such as power supply and measurement of both static and dynamic pressures become more problematic for wearable pressure sensors. Considering the current existing issues, it is in urgent demand on developing self-powered pressure sensors with high sensitivity for reliable detection of both static and dynamic stimuli.

Here, we demonstrate a novel self-powered electronic skin sensor to solve the issues mentioned above. To obtain the stable and durable power supply, a self-powered piezoresistive pressure sensor is designed based on the redox reaction-induced electricity between the Al electrode and graphite/PDMS composite (GPC) electrode with the electrolyte participating. It has been demonstrated that bio-inspired design is an effective strategy for the enhancement of sensitivity and detection range for skin sensors. Park et al. developed the fingerprint inspired patterns and interlocking microstructures in ferroelectric film to enhance the piezoelectric, pyroelectric, and piezoresistive sensing in temperature and pressure.<sup>51</sup>

Mimicking the hierarchical structures of natural plants, bio-inspired TENGs as self-powered e-skin sensors were reported by Yao et al. for tactile sensing.<sup>48</sup> Meanwhile, motivated by the microstructures underlying the epidermis, the bio-inspired graphite/PDMS sensing films are laminated face-to-face mimicking the receptors under the epidermis to sense the external pressures which can deform the microstructures of the composite films and thereby changing the current output of the pressure sensors. This strategy endows the novel self-powered electronic skin sensor with the ability to detect not only the dynamic forces but also the static ones. Based on the redox-induced electricity and the double-layer structured composite geometry, the sensors show remarkable device properties including an ultrahigh sensitivity ( $\sim 10^3 \text{ kPa}^{-1}$ ) and a wide detection range (0.02–30 kPa). Noteworthy, to our best of knowledge, it has been rarely reported that redox-induced electricity based self-powered pressure/tactile sensors achieve a high sensitivity for both static and dynamic pressure detection simultaneously. Additionally, the device exhibits fast response/relaxation speed, outstanding durability, and excellent detection resolution as well. Benefiting from the excellent pressure-sensing performance, our sensors are not only applicable to healthcare monitoring, human motion detection, communications, and e-skin, but also present a new insight into the development of high-performance self-powered flexible electronics as well.

## **EXPERIMENTAL SECTION**

**Materials.** Graphite powder was purchased from Beijing Jinlong Tetan Technology Co., Ltd. PDMS base agent and crosslinker were obtained from DOW. Sodium chloride (NaCl, 99%) was bought from Sigma Aldrich. Polyethylene terephthalate (PET) substrates, PET substrates coated with indium tin oxide (ITO, 100 nm), copper wires and 3M double side tape were all purchased from South China Science and Technology Co., Ltd. Sandpapers were bought from market. All the chemicals were used as received without further purification.

**Fabrication of the bio-inspired composite films.** The piezoresistive composite films with hierarchical structures were prepared as following. Firstly, the graphite powder was added

into the PDMS prepolymer followed by vigorous stir to obtain the graphite/PDMS ink. The graphite mass percentage in the prepared composite ink varied from 10 wt% to 60 wt% with an interval of 10 wt%. For the PDMS prepolymer, the mass ratio between the base and the crosslinker is 10:1. Secondly, the composite ink was brushed onto the surface of the sandpaper which was fixed to the platform of a roller printer by using PI tapes and a piece of PET or ITO/PET sheet was then covered on top. Graphite/PDMS composite films with different surface microstructures were prepared using sandpaper with different roughness (#80, #120, and #220). After that, the composite ink was uniformly spread between the sandpaper and the PET or ITO/PET substrates after the roller bar moved from one side of the substrate to the other side. The thickness of piezoresistive films could be controlled by inserting spacers between the template and PET or ITO/PET substrate. Subsequently, the composite ink films together with the template and PET or ITO/PET substrates were sandwiched between two steel plates followed by curing at 100 °C for 1 h. Finally, hierarchically microstructured piezoresistive composite films were obtained after the removal of sandpaper template. The fabrication procedure of planar graphite/PDMS composite film is similar with that of the microstructured film except that the sandpaper template is replaced by a PET substrate.

**Preparation of PDMS spacers.** Firstly, PDMS prepolymer was prepared by mixing PDMS base agent and related crosslinker at a weight ratio of 10:1 followed by mechanically stirred for 10 min to get uniform mixture. Afterwards, the air bubbles in the mixture were removed by placing the PDMS prepolymer in a vacuum oven under a low pressure. Next, the preparation process of the PDMS films was similar with that of the piezoresistive composite films using the bar-assisted printing method. The PDMS films were fabricated between two pieces of PET substrates instead of the sandpaper and ITO/PET. After thermally annealed at 100 °C for 1 h, the PDMS film solidified and was then cut into 2 cm × 2 cm squares with a 1.5 cm × 1.5 cm open square in the middle using a doctor blade.

**Preparation of the NaCl electrolyte solution.** Proper amount of NaCl powder was added into deionized water (DI-water) to obtain the electrolyte solution with a concentration of 5 wt%.

**Fabrication of the self-powered skin sensor and 4 × 4 sensor arrays.** Firstly, the Al tape was cut into rectangle shapes (2 cm × 2.5 cm) followed by attached to the PET substrate. Then, the PDMS spacer was laminated on top of the Al electrode and the PDMS prepolymer was used to seal the possible gap between the Al electrode and the spacer to avoid the electrolyte solution leakage. The PDMS prepolymer solidified after thermally treated at 100 °C for 1 h to ensure a rigid attachment between Al electrode and the spacer. Next, proper amount of NaCl electrolyte solution was filled in the open square by using a dropper. After that, the piezoresistive composite film (the microstructured side opposite the electrolyte solution) was covered on top of the spacer with PDMS prepolymer in between and the prepolymer solidified at room temperature after 12 h. Subsequently, another microstructured graphite/PDMS composite film on a ITO/PET substrate was cut into rectangle shapes (2 cm × 2.5 cm for the ITO/PET, and 2 cm × 2 cm for the composite film) and assembled to the pressure sensor using the 3M double side tape with the microstructured surface facing the bottom composite film. Finally, copper wires were connected to the Al and ITO electrodes for external connections. The pressure sensing arrays were constructed based on the conventional crossbar configuration, which was composed of 16 sensing units. The fabrication procedure for every sensing unit of the pressure sensor arrays was the same as that of the single pressure sensor device.

**Characterization and measurement.** The microstructures and morphology of the graphite/PDMS piezoresistive composite films and sandpaper template were investigated by using scanning electron microscope (SEM, JEOL, JSM-6490). The surface roughness of the microstructured piezoresistive film was characterized using a 3D Surface Profiler (Wyko NT9300). The electrical signals of the self-powered pressure sensor and pressure sensor

arrays were measured using Keithley 2612A. The mechanical tests were performed by using a mechanized vertical test stand (Mark 10 ESM 303) in combination with a force gauge (Mark 10 M5-12).

## **RESULTS AND DISCUSSION**

### **Fabrication of the self-powered electronic skin sensor**

Detailed device fabrication procedures of the electronic skin sensors are shown in Figure S1 (Supporting Information). The first step towards assembling the skin sensors is the fabrication of the bio-inspired composite films. As depicted in Figure S1a, the microstructured composite film is prepared by a bar-assisted printing process. After that, the PET substrate, Al electrode, and PDMS spacer were assembled layer by layer as shown in Figure S1b. After NaCl electrolyte solution was filled into the well of the spacer, the bio-inspired composite film as cathode was covered on top with the microstructured surface opposite the electrolyte solution and sealed with PDMS prepolymer. Another piece of composite film on ITO/PET substrate was then laminated on top with the microstructured side facing the bottom composite film and double side tape was inserted between these two composite layers near the edges, where the double side tape can laminate these two layers together and works as a spacer to minimize the initial contact between these two piezoresistive composite films. It should be noticed that the piezoresistive film conductivity could be well controlled by adjusting the graphite filler mass ratio in the composite inks. The sensitivity of the redox-induced electricity powered skin sensors based on the bio-inspired GPC films with varied graphite ratios is shown in Figure S2. A very low sensitivity of the sensor is obtained when the graphite concentration is less than 20 wt%, which may be due to the intrinsic poor conductivity of the piezoresistive composite films with low graphite concentrations. After the graphite concentration is up to 30 wt%, the pressure sensitivity of the sensors increases obviously with the increased graphite concentration. Although the sensors based on 50 wt% and 60 wt% composite films show higher pressure sensitivity, the viscosities of 50 wt% and 60 wt% composite inks increase a

lot, which is not suitable for the future mass production. With the tradeoff between the sensitivity of the skin sensors and fabrication feasibility of the piezoresistive composites, composite films with 40 wt% graphite concentration are selected for sensors in this work unless otherwise specified. As shown in the schematic diagram of biological skin (**Figure 1a**), the surface of the dermis is composed of various microstructures and many receptors distribute in the dermis, which can detect the external stimuli. Inspired by the structure and function of biological skin, a redox-induced electricity powered electronic skin sensor is developed as depicted in Figure 1b. The hierarchically microstructured surface enables the sandpaper to be an excellent candidate template for preparing bio-inspired microstructures. Sandpaper is employed as template in this work to obtain the microstructured piezoresistive composite films. The surface microstructures of the sandpaper template and the prepared composite film were characterized with a scanning electron microscope (SEM), respectively. As depicted in Figure 1c, the sandpaper template shows a rough surface and ridged microstructures, mimicking the microstructures of human epidermis. As observed in Figure 1d, the piezoresistive composite film could well duplicate the microstructures from the template and reserving the rough surface, proving a feasible way to obtain bio-inspired hierarchical microstructures. Additionally, the surface 3D profile of the composite film was characterized as shown in Figure 1e, further demonstrating the relatively rough and hierarchically structured surface of the composite film.

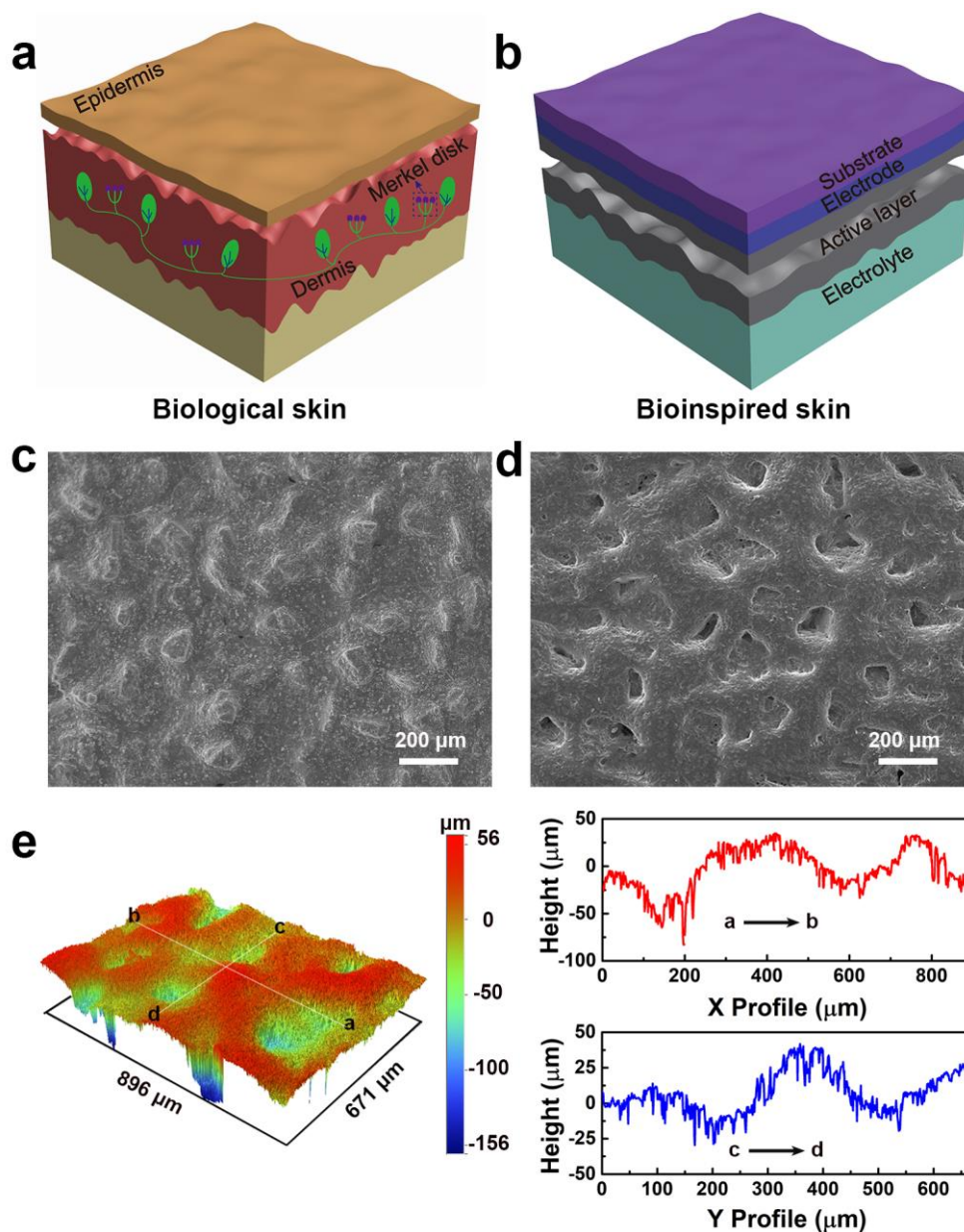


**Figure 1.** (a) and (b) Schematic diagrams of biological skin and bio-inspired electronic skin, respectively. (c) SEM image of sandpaper template and (d) SEM image of the bio-inspired composite film. (e) Surface height in 3D image of bio-inspired composite film and the cross-sectional heights measured along the lines (ab and cd) as depicted in the 3D image.

### Transduction mechanism of the self-powered electronic skin sensor

The redox-induced electricity powered electronic skin sensors are constructed according to the following transduction mechanism. The mechanism of generating electricity is based on the electrochemical principles that electrons and holes could be induced spontaneously at the surface of graphite and aluminum electrodes because of their differences in chemical potential

with the electrolyte participating.<sup>52</sup> When the anode and cathode are externally connected, reduction reaction occurs at the interface between the graphite/PDMS film and the electrolyte, where the oxygen molecules dissolved in the aqueous electrolyte could capture electrons and then turn into hydroxyl ions ( $3\text{O}_2 + 6\text{H}_2\text{O} + 12\text{e}^- \rightarrow 12\text{OH}^-$ ). Oxidation reaction takes place at the interface of aluminum and electrolyte, and the Al atoms lose electrons followed by turning into aluminum hydroxide ( $4\text{Al} - 12\text{e}^- + 12\text{OH}^- \rightarrow 4\text{Al}(\text{OH})_3$ ). The open-circuit voltage in this sensing system is only determined by the redox potential of anode and cathode electrodes, which means the battery part can supply a constant open-circuit voltage. According to Ohm's law, the output current in the circuit can be changed by changing the loading resistance. Therefore, the external pressure can be evaluated by the output current. As shown in **Figure 2a**, without external pressure, these two piezoresistive composite layers are partially contacted and result in a high loading resistance, which obstructs the electrochemical redox reaction and in turn a low current. The applied external pressure can compress the surface microstructures of the piezoresistive composite films, resulting in a reduced loaded resistance, which boosts up the redox reaction and results in an enhanced output current. Meanwhile,  $\text{Na}^+$  and  $\text{Cl}^-$  ions in the electrolyte solution move towards the cathode and anode, respectively. Self-powered pressure sensors based on three types of graphite/PDMS composite films developed by sandpapers with different roughness (#80, #120, and #220) were fabricated. The relative current change to applied pressure of these three types of pressure sensor were investigated as shown in Figure S3. The devices developed from the #80, # 120, and #220 sandpapers are denoted as "Sensor A", "Sensor B", and "Sensor C", respectively. Sensor B shows the higher sensitivity compared with Sensor A and C. As depicted in Figure S3, the micro-humps with smaller feature size (#220) lead to a lower sensitivity due to limited variation of contact area and extra conductive paths when the device is under external pressure. For Sensor A, the

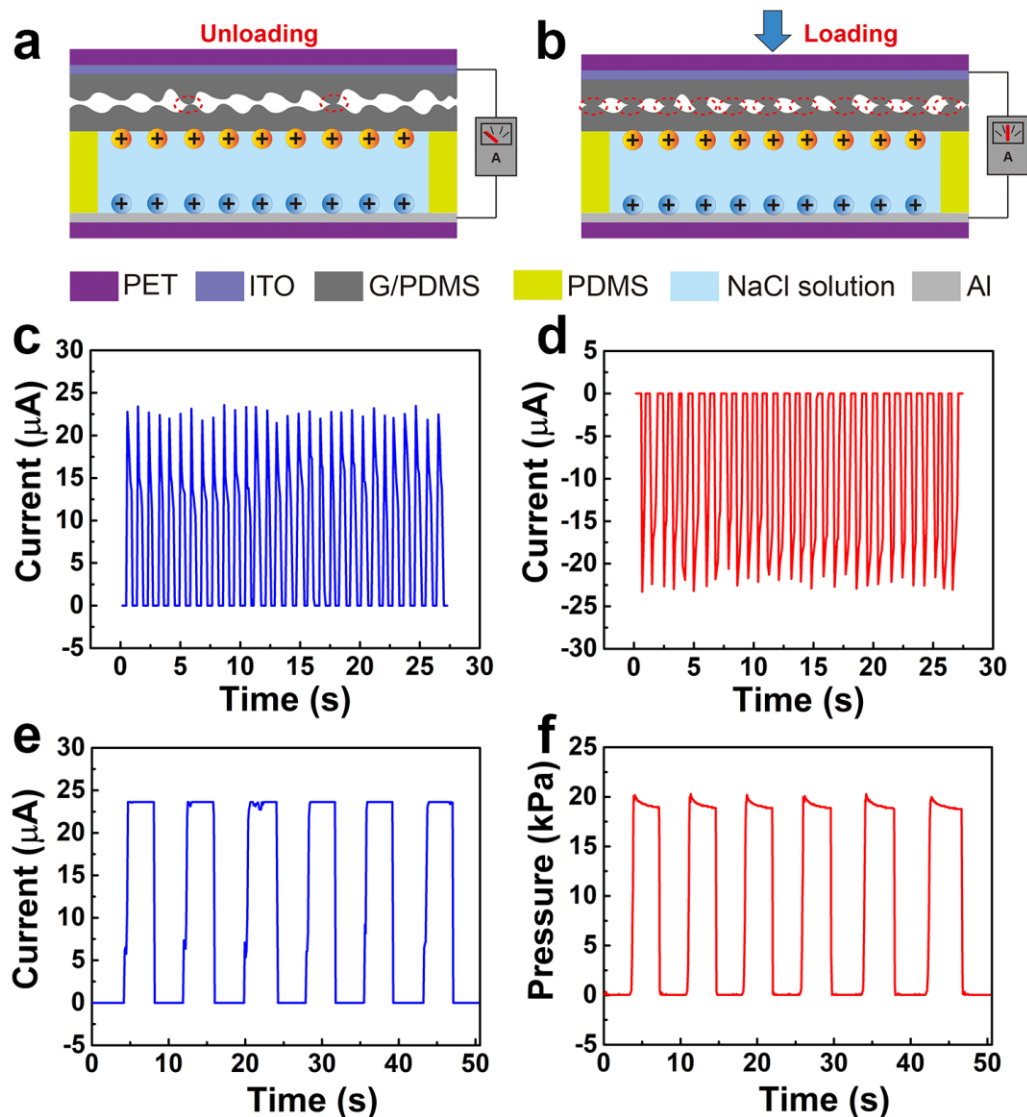


**Figure 2.** Schematic diagrams showing the sensing mechanism of the self-powered skin sensors (a) without external pressure and (b) with external pressure. (c) Current responses of the self-powered skin sensor to dynamic-cyclic pressure  $\sim 20$  kPa and (d) the connection is reversed. (e) Current responses to static-cyclic pressure  $\sim 20$  kPa and (f) the relevant applied static pressure measured by force gauge.

variation in the height of the microhumps is large so that the formation of extra conductive paths may require a higher pressure and results in decreased device sensitivity. In this work, all the characterizations are for #120 sandpaper developed composite film based self-powered pressure sensors and arrays unless with special remarks. Figure 2c-f shows the electrical performance of the sensor in detecting both dynamic and static pressures. For the dynamic measurement as depicted in Figure 2c and d, the pressure sensor shows an output current of

22  $\mu\text{A}$  under a pressure of 20 kPa. When the connections of the sensor to our measurement equipment are reversed, the direction of the current is just reversed but the current values keep almost the same. Significantly, the electronic skin sensors show excellent performance in reliable detection of static pressures as shown in Figure 2e and f, which is rarely reported for the self-powered pressure sensors. As noticed in Figure 2e, the sensor shows a high output current when a constant pressure is applied to the sensor as shown in Figure 2f and vice versa. The above results demonstrate that our self-powered skin sensors show high performance in detecting both dynamic and static pressures. A comparing schematic diagram showing the advances of our self-powered skin sensor to the typical nanogenerators is exhibited in Figure S3 (Supporting Information). For the static pressure detection by output current measurement, the typical nanogenerators can not reveal the period of the applied static pressure as depicted in Figure S4a, which obstructs their application in spatial pressure distribution mapping. However, due to the difference in sensing mechanism of our self-powered skin sensor to the typical nanogenerators, the static pressure applied on the device can be well detected as shown in Figure S4b. Additionally, the output voltage of the self-powered skin sensors was characterized as shown in Figure S5 (Supporting Information). The device provides a constant output voltage regardless of the applied pressure. This is because the power supply for our sensor is based on the redox-induced electricity and the output voltage is only determined by the redox potential of anode and cathode electrodes, which has been widely discussed in battery devices.<sup>53,54</sup> Furthermore, the electricity source without the upper graphite/PDMS sensing film was fabricated. The short-circuit current ( $I_{\text{SC}}$ ) and open-circuit voltage ( $V_{\text{OC}}$ ) of the electricity source are measured as shown in Figure S6, demonstrating a  $I_{\text{SC}}$  and  $V_{\text{OC}}$  of 93  $\mu\text{A}$  and 0.92 V, respectively. Besides, the output current of the sensor is continuously measured for about 5 hours with applying a constant pressure of 30 kPa to check its current stability as depicted in Figure S7 (Supporting Information). It is observed that there is no obvious current recession in the testing process, which is attributed to the relatively slow rate of redox reaction in the electrode because of the high resistance of the composite films.

Furthermore, the collected current output of the sensor up to 60 days is shown in Figure S8 (Supporting Information) and about 10.7% current decay was observed after 60 days. Because the consumption of the aluminum electrode may influence the lifetime of the redox couple/chemical energy, we thus checked the aluminum electrode consumption after 60 days and the consumption is about 16.2%, which demonstrates the redox reaction in our sensor is with a slow process. The life time and sensing performance of our sensor can satisfy most of the wearable applications in health monitoring etc. Additionally, the static output current of the pressure sensor is less than 1 nA when no additional pressure is applied to the device, so the redox-induced electricity powered sensors are expected to work with a much longer lifetime.

### **Characterization of the self-powered electronic skin sensor**

Based on the transduction mechanism, different pressures are applied to the device to explore its sensitivity in sensing pressures. The sensitivity ( $S$ ) of the self-powered skin sensors can be defined as  $S = \delta(\Delta I / I_0) / \delta P$ , where  $\Delta I$ ,  $I_0$ , and  $P$  denote the change in current, initial current, and applied pressure, respectively. The relative current change as a function of static pressure is depicted in **Figure 3a** and the sensitivity corresponds to the slope of the curve. We observe that the relative current change increases with the external pressures, which should be ascribed to the more close contact between these two piezoresistive composite films under larger external pressures. The sensitivities are estimated as  $4.2 \times 10^3$  and  $1.1 \times 10^3$   $\text{kPa}^{-1}$  for the sensing range of 0-4 and 4-30 kPa, respectively. The higher sensitivity in the relative low detection range of 0-4 kPa is possible as a result of the increased conductive pathways with the external pressure, which induces an obvious current change. It is noticed that the sensitivity decreases a little when the pressure is beyond 4 kPa, which is because the number of the conductive pathways are almost saturated in the high sensing range and the pressure sensitivity should be mainly ascribed to the increased contact area between these two piezoresistive composite films. Additionally, current response of the self-powered skin sensor

to dynamic pressures was also characterized as shown in Figure S9, indicating the similar sensitivity and linear sensing range as the static measurement. It should be noticed that the sensitivity of our self-powered skin sensor is greatly improved compared with previously reported piezoresistive pressure sensors,<sup>11,55-58</sup> which may be attributed to the employment of the double side tape as the spacer when assembling the device. The employment of spacers between the composite films enables the reduction of conductive pathways when there is no external pressure loaded on the sensor device, which can minimize the static power consumption and boost up the pressure sensitivity simultaneously.

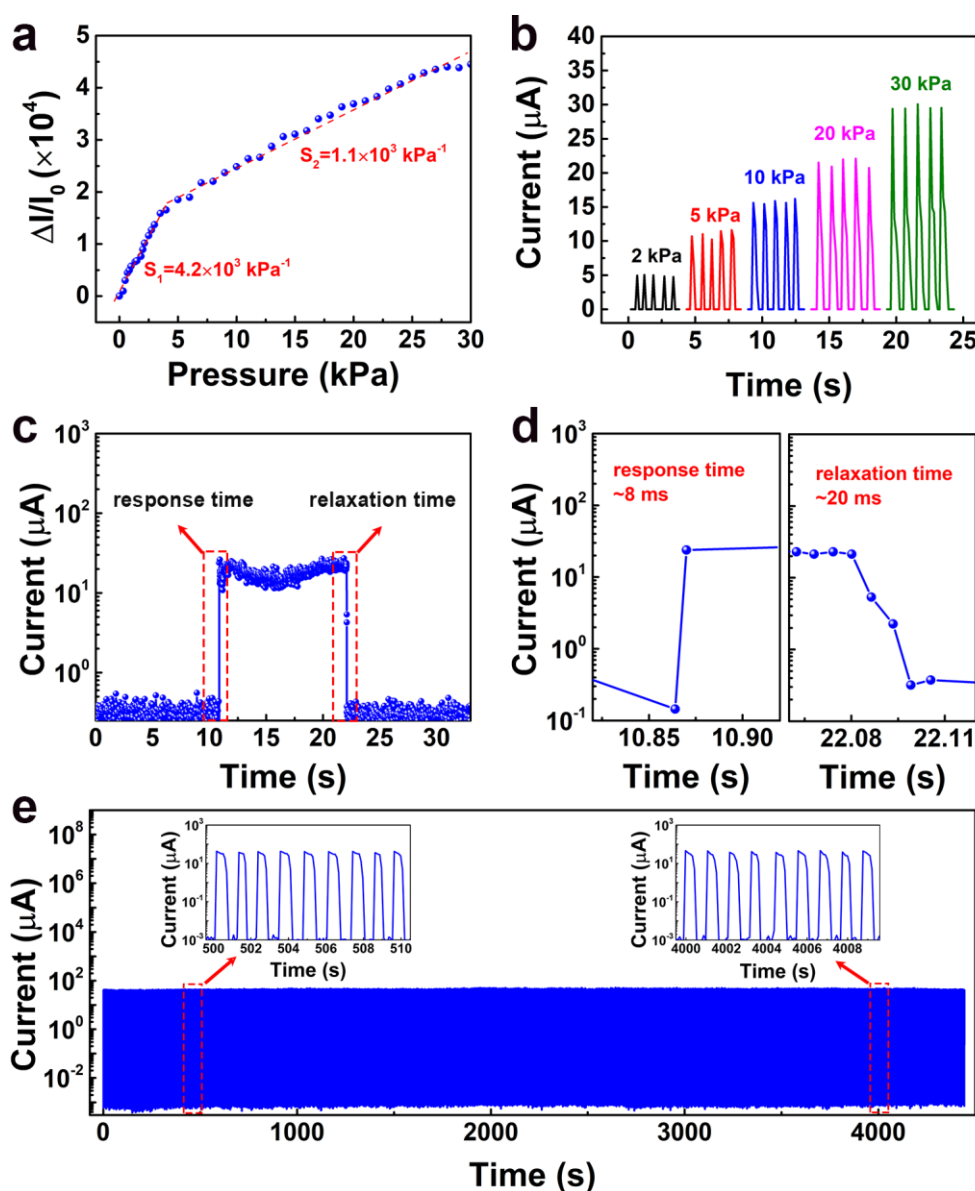


**Figure 3.** Pressure sensing characteristics of the self-powered pressure sensors based on redox-induced electricity. (a) The relative change of current to different pressures. (b) The current responses to different cyclic pressures. (c) Current responses of pressure sensor in the process of loading/unloading a pressure of 20 kPa. (d) Enlarged view of the curves in c showing the response and relaxation time. (e) The durability of the self-powered pressure sensors to cyclic pressures over 4000 cycles. The insets show the enlarged view of the current responses at the beginning and in the end of the test.

The pressure related measurements of the self-powered skin sensors were performed in detail. First, cyclic current response to various dynamic pressures (2, 5, 10, 20, and 30 kPa) was measured as presented in Figure 3b. The result shows that the output current increases with enlarging the applied pressure and the sensor could efficiently distinguish different dynamic pressures by the current difference in altitudes. A larger loading pressure induces a more close contact between these two piezoresistive composite layers, leading to a larger output current. Limit of detection (LOD), the minimum pressure that the sensor can detect, is a key parameter to assess the sensing performance of the sensor. As shown in Figure S10 (Supporting Information), in order to define the LOD of our self-powered skin sensor, a piece of plant leaf (20 mg) was loaded/unloaded onto the device to check its current response. The inset in Figure S10 is the photograph of a plant leaf on top of the sensor. Interestingly, our redox-induced electricity based skin sensor could effectively distinguish the subtle pressure changes generated in the process of loading and unloading the plant leaf. The effective contact area is around 1 cm<sup>2</sup>, indicating a LOD around 20 Pa, which is comparable to the previously reported pressure sensors.<sup>25,59</sup> For pressure sensors, response speed to external pressures is another crucial parameter evaluating the sensing performance. As shown in Figure 3c, to investigate the response and relaxation speed, the sensor was characterized by loading/unloading a pressure of 20 kPa. Remarkably, the response and relaxation time of the self-powered sensor is extracted from Figure 3d as 8 and 20 ms, respectively, which is faster than that of biological skin (~50 ms),<sup>60</sup> demonstrating the great potential of our self-powered sensor for the next-generation e-skin. Furthermore, as depicted in Figure 3e, the long-term durability more than

4000 cycles was performed by loading/unloading a constant pressure of 20 kPa. No obvious recession is perceived at the the end of the test and the fluctuation in current altitude is less than 5 percent during the entire testing process. An enlarged view of the output current curves picked at the beginning and end of the testing process is shown in the inset of Figure 3e, of which almost identical current amplitude was well maintained for all the loading/unloading cycles, further demonstrating the intriguing potential of our sensor for next-generation flexible electronics. Beside the durability, ambient stability of the skin sensor is also a crucial factor influencing the practical applications. To investigate the ambient stability of the sensors, the devices were stored in the ambient condition (H~80%, T~25 °C) for 6 months and the durability of the pressure sensor to cyclic external pressures was characterized afterwards. As shown in Figure S11 (Supporting Information), we observe that the pressure sensor sustains a stable output current after stored in the ambient condition for such long time, which further demonstrates the potential applications of our self-powered skin sensors for future wearable and portable electronics.

### **Applications of the self-powered electronic skin sensor**

Pressure sensors have been demonstrated the great potential application in real-time monitoring the human wrist pulses.<sup>50</sup> A self-powered pressure sensor is much more appealing than those requiring an external power supply, which enables the pressure sensing system to be more compact, smart, and environmentally friendly. Human arterial pulse is a key indicator which can monitor the health condition of the cardiovascular system to prevent angiocardopathy. As a result of the high sensitivity as well as the fast response speed, our self-powered pressure sensors have been demonstrated the potential application in health monitoring by detecting the wrist pulses as shown in **Figure 4a** and b. The photograph of the pressure sensor affixed onto the arterial wrist of a volunteer is exhibited in the inset of Figure 4b. It is observed from Figure 4a that high-resolution signal-to-noise waveform of the wrist pulses is obtained by our self-powered pressure sensors. The counted heart beat rate is around

72 beats per minute (bpm), indicating that the heart beat rate of the adult is in the normal range of 60~100 bpm. Enlarged view of the wrist pulse waveform is shown in Figure 4b, which illustrates that three typical peaks are clearly revealed by our sensor. The systolic augmentation index (AI), defined as  $AI = (P1-P2)/P1$ , is used to diagnose arterial stiffness to analyze the health condition of the cardiovascular system, which can be obtained from Figure 4b.<sup>61</sup> The result proves that our sensor has the great potential application in wearable and portable health monitoring electronics.

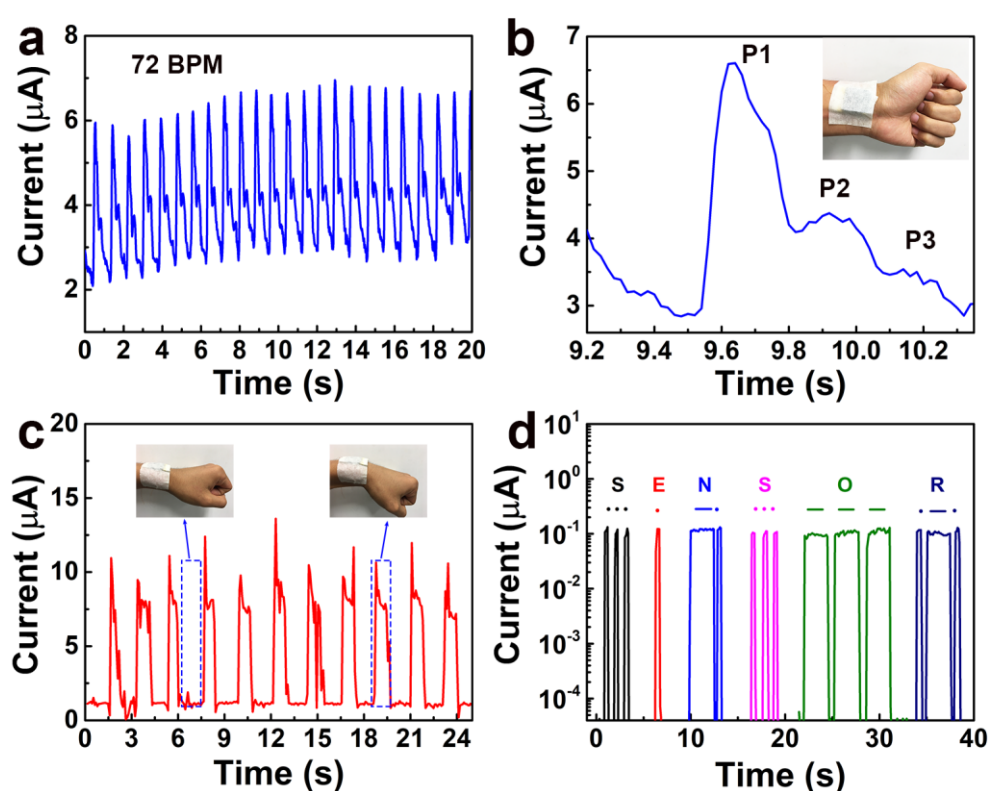


**Figure 4.** (a) Arterial wrist pulse detected by the self-powered pressure sensor. (b) The enlarged view of the picked waveform from (a). The inset is the photograph of the pressure sensor attached on a human wrist. (c) The current responses of the pressure sensor to different bending states of human wrist. The insets are the photographs showing the bending states of human wrist. (d) The application of the sensor in generating Morse code “SENSOR”.

As another application illustration, the self-powered pressure sensor was affixed onto the wrist of a volunteer to monitor the bending of the wrist. As depicted in Figure 4c, a stretched state of the wrist (the left inset in Figure 4c) corresponds to a small current of the sensor,

which is because of the very few conductive pathways between these two piezoresistive composite films are formed in this state. An obviously enhanced current is obtained when the wrist is in bending state (the right inset of Figure 4c). This is attributed to the increased conductive pathways and the enlarged contacting area when the wrist is bended. The above results prove that our electronic skin sensors have the great potential in detecting human body motions.

The Morse code has been used for decades in communication, which is one of the fastest ways to transmit messages over a long distance in the late 1800s. For international Morse codes, different combinations of dashes or dots represent different alphabets. Thanks to its ability in detecting both dynamic and static pressures, our skin sensor is an excellent candidate for Morse code generation and transmission. Here, according to the period of the pressure applied onto the sensors, output current with a sharp or flat peak was generated and transmitted in this process. A sharp output current peak corresponds to a dot while a flat output current represents a dash. The Morse codes “SENSOR” were generated and transmitted based on the mechanism discussed above. An encoding process was performed by pressing the self-powered pressure sensor with different periods of pressing and a decoding process was carried out by collecting the current signals as depicted in Figure 4d. The above results demonstrate that our self-powered pressure sensor has the potentials as a Morse code generator, indicating the possibility of our device to be developed into real products for applications in communication systems.

### **Spatial pressure distribution mapping**

On the basis of the redox-induced electricity powered individual sensor, a  $4 \times 4$  self-powered pressure sensor array was fabricated to demonstrate its application in mapping the spatial pressure distribution. As far as we concerned, it is also the first demonstration of the redox-induced electricity based pressure sensor arrays for detecting the spatial pressure distribution. The detailed fabrication process of the pressure sensor arrays is described in the experimental

section. As a demonstration of concept, different objects were placed on top of the pressure sensor arrays and the current responses of the pressure sensing cells were measured accordingly. When four weights (5, 10, 20, and 20g) were randomly placed on top of the sensing cells as shown in the schematic diagram in **Figure 5a** (the photograph is shown in Figure S12a, Supporting Information), the pressure distribution could be well detected and similar maps in current are correspondingly shown in Figure 5c. Furthermore, as presented in Figure 5b and S12b, when a glass ring (28.6 g) was put on top of the sensing cells, the shape of the ring was well revealed by the current mapping as shown in Figure 5d. The pressure distribution detected by the self-powered pressure sensor arrays can be applied to monitor the planar feet pressure distribution, prosthetics, and mapping the shape of the objects, etc. The detection resolution and accuracy are expected to be further improved by minimizing the area of the sensing unit.

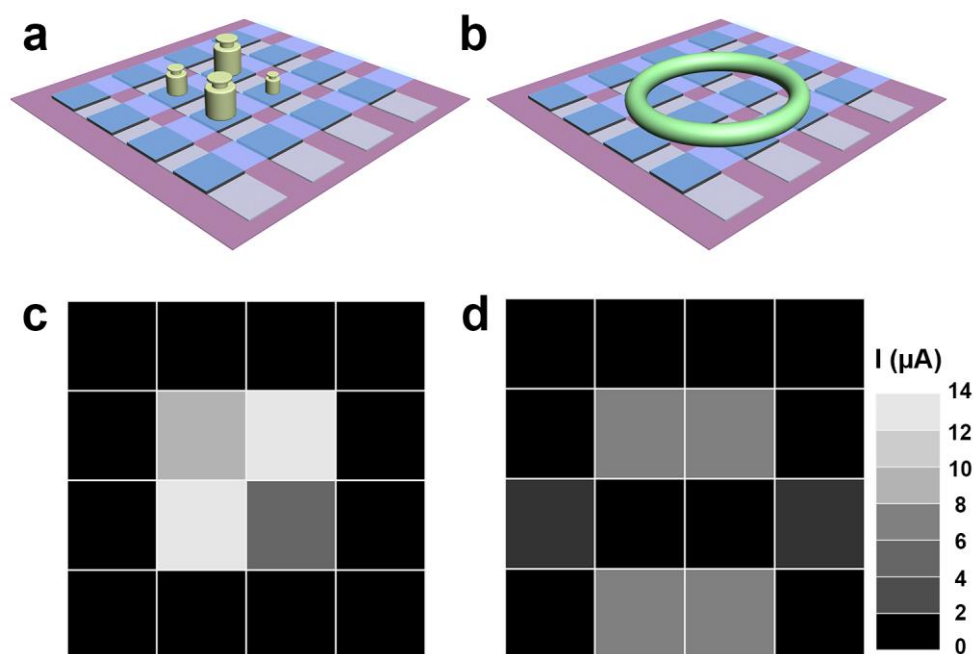


**Figure 5.** Self-powered pressure sensor arrays in mapping the spatial pressure distribution. Schematics of the pressure sensor arrays with (a) 4 weights (5, 10, 20, and 20 g) and (b) a glass ring (28.6 g) on top. (c) and (d) The corresponding current maps for (a) and (b), respectively.

## CONCLUSIONS

In summary, a feasible strategy is presented to develop the self-powered and bio-inspired electronic skin sensors. The self-powered devices exhibit a high performance in sensing both dynamic and static pressures, including an ultrahigh sensitivity of  $4.2 \times 10^3 \text{ kPa}^{-1}$ , a LOD of 20 Pa, a fast response speed of 8 ms, and excellent durability over 4000 cycles. Remarkably, as a result of the ultrahigh sensitivity and fast response speed, the redox-induced electricity powered skin sensors have been demonstrated the ability to obtain high resolution signal-to-noise wrist pulse waveforms in real time. Additionally, their applications in monitoring human body motions and generating Morse code for communication have been proved. Furthermore, the self-powered pressure sensor arrays are capable to map the spatial pressure distribution, demonstrating the potential application for e-skin and prosthetics. Moreover, no sophisticated equipment or costly materials are involved in the process of fabricating the flexible self-powered skin sensors or arrays, which fulfills the requirement for next-generation low-cost wearable electronics. In this work, we not only develop a novel self-powered electronic skin sensor, but also propose a new strategy to achieve the self-powered flexible electronics.

## ASSOCIATED CONTENT

### Supporting Information

Supporting Information Available: Detailed information about fabrication of the bio-inspired composite film and self-powered electronic skin, characterization of the effect of graphite concentration to pressure sensitivity, the effects of surface roughness of graphite/PDMS on pressure sensitivity, schematic illustration of the difference in sensing mechanism of our self-powered sensor to the reported nanogenerator based sensors, characterization of output voltage to applied pressures, output current and voltage of the electricity power without pressure sensing layer, durability characterization of the electronic skin, long-term output current characterization up to 2 months, dynamic pressure sensitivity, characterization of limit

of detection, ambient stability of the sensor, and photographs of the sensor arrays for pressure distribution detection. This material is available free of charge via the Internet at <http://pubs.acs.org>.

Figures S1-S12 (PDF)

## **AUTHOR INFORMATION**

### **Corresponding Author**

Tel: 86-852-34422729, Fax: 86-852-34420538

\*E-mail: [val.roy@cityu.edu.hk](mailto:val.roy@cityu.edu.hk)

### **Author Contributions**

‡Q. J. Sun and X. J. Zhao contributed equally to this work.

### **Notes**

The authors declare no competing financial interest.

## **ACKNOWLEDGMENT**

The authors acknowledge the grant from the Research Grant Council of HKSAR (Grant No. T42-103/16N) and Applied Research Grant from City University of Hong Kong (Grant No. 9667145).

## REFERENCES

- (1) Trung, T. Q.; Lee, N. -E. Flexible and Stretchable Physical Sensor Integrated Platforms for Wearable Human-Activity Monitoring and Personal Healthcare. *Adv. Mater.* **2016**, *28*, 4338-4372.
- (2) Boutry, C. M.; Nguyen, A.; Lawal, Q. O.; Chortos, A.; Gagné, S. R.; Bao, Z. A Sensitive and Biodegradable Pressure Sensor Array for Cardiovascular Monitoring. *Adv. Mater.* **2015**, *27*, 6954–6961.
- (3) Xiao, Z.; Zhou, W.; Zhang, N. ; Zhang, Q.; Xia, X.; Gu, X.; Wang, Y. ; Xie, S. All-Carbon Pressure Sensors with High Performance and Excellent Chemical Resistance. *Small* **2019**, *15*, e1804779.
- (4) Zang, Y.; Zhang, F.; Di, C.-A.; Zhu, D. Advances of Flexible Pressure Sensors Toward Artificial Intelligence and Health Care Applications. *Mater. Horiz.* **2015**, *2*, 140-156.
- (5) Wang, Z.; Guan, X.; Huang, H.; Wang, H.; Lin, W.; Peng, Z. Full 3D Printing of Stretchable Piezoresistive Sensor with Hierarchical Porosity and Multimodulus Architecture. *Adv. Funct. Mater.* **2019**, *29*, 1807569.
- (6) Lee, J. H.; Hwang, J. Y.; Zhu, J.; Hwang, H. R.; Lee, S. M.; Cheng, H.; Lee, S. H.; Hwang, S. W. Flexible Conductive Composite Integrated with Personal Earphone for Wireless, Real-Time Monitoring of Electrophysiological Signs. *ACS Appl. Mater. Interfaces* **2018**, *10*, 21184-21190.
- (7) Wang, X.; Liu, Z.; Zhang, T. Flexible Sensing Electronics for Wearable/Attachable Health Monitoring. *Small* **2017**, *13*, 1602790.
- (8) Jiang, S.; Yu, J.; Xiao, Y.; Zhu, Y.; Zhang, W. Ultrawide Sensing Range and Highly Sensitive Flexible Pressure Sensor Based on a Percolative Thin Film with a Knoll-like Microstructured Surface. *ACS Appl. Mater. Interfaces* **2019**, *11*, 20500-20508.

- (9) Song, Y.; Chen, H.; Su, Z.; Chen, X.; Miao, L.; Zhang, J.; Cheng, X.; Zhang, H. Highly Compressible Integrated Supercapacitor-Piezoresistance-Sensor System with CNT-PDMS Sponge for Health Monitoring. *Small* **2017**, *13*, 1702091.
- (10) Cao, R.; Pu, X.; Du, X.; Yang, W.; Wang, J.; Guo, H.; Zhao, S.; Yuan, Z.; Zhang, C.; Li, C.; Wang, Z. L. Screen-Printed Washable Electronic Textiles as Self-Powered Touch/Gesture Tribo-Sensors for Intelligent Human-Machine Interaction. *ACS Nano* **2018**, *12*, 5190-5196.
- (11) Pyo, S.; Lee, J.; Kim, W.; Jo, E.; Kim, J. Multi-Layered, Hierarchical Fabric-Based Tactile Sensors with High Sensitivity and Linearity in Ultrawide Pressure Range. *Adv. Funct. Mater.* **2019**, *29*, 1902484.
- (12) Chen, M.; Li, K.; Cheng, G.; He, K.; Li, W.; Zhang, D.; Li, W.; Feng, Y.; Wei, L.; Li, W.; Zhong, G.; Yang, C. Touchpoint-Tailored Ultrasensitive Piezoresistive Pressure Sensors with a Broad Dynamic Response Range and Low Detection Limit. *ACS Appl. Mater. Interfaces* **2019**, *11*, 2551-2558.
- (13) Xie, M.; Hisano, K.; Zhu, M.; Toyoshi, T.; Pan, M.; Okada, S.; Tsutsumi, O.; Kawamura, S.; Bowen, Ch. Flexible Multifunctional Sensors for Wearable and Robotic Applications. *Adv. Mater. Technol.* **2019**, *4*, 1800626.
- (14) Wang, J.; Lin, M. - F.; Park, S.; Lee, P. S. Deformable Conductors for Human-Machine Interface. *Mater. Today* **2018**, *21*, 508-526.
- (15) Gerratt, A. P.; Michaud, H. O.; Lacour, S. P. Elastomeric Electronic Skin for Prosthetic Tactile Sensation. *Adv. Funct. Mater.* **2015**, *25*, 2287-2295.
- (16) Liang, Z.; Cheng, J.; Zhao, Q.; Zhao, X.; Han, Z.; Chen, Y.; Ma, Y.; Feng, X. High-Performance Flexible Tactile Sensor Enabling Intelligent Haptic Perception for a Soft Prosthetic Hand. *Adv. Mater. Technol.* **2019**, *4*, 1900317.

- (17) Lee, W. W.; Tan, Y. J.; Yao, H.; Li, S.; See, H. H.; Hon, M.; Ng, K. A.; Xiong, B.; Ho, J. S.; Tee, B. C. K. A Neuro-Inspired Artificial Peripheral Nervous System for Scalable Electronic Skins. *Sci. Robot.* **2019**, *4*, eaax2198.
- (18) Zhang, C.; Ye, W. B.; Zhou, K.; Chen, H. Y.; Yang, J. Q.; Ding, G.; Chen, X.; Zhou, Y.; Zhou, L.; Li, F.; Han, S. T. Bioinspired Artificial Sensory Nerve Based on Nafion Memristor. *Adv. Funct. Mater.* **2019**, *29*, 1808783.
- (19) Chhetry, A.; Kim, J.; Yoon, H.; Park, J. Y. Ultrasensitive Interfacial Capacitive Pressure Sensor Based on a Randomly Distributed Microstructured Iontronic Film for Wearable Applications. *ACS Appl. Mater. Interfaces* **2019**, *11*, 3438-3449.
- (20) Luo, Y.; Shao, J.; Chen, S.; Chen, X.; Tian, H.; Li, X.; Wang, L.; Wang, D.; Lu, B. Flexible Capacitive Pressure Sensor Enhanced by Tilted Micropillar Arrays. *ACS Appl. Mater. Interfaces* **2019**, *11*, 17796-17803.
- (21) Qiu, Z.; Wan, Y.; Zhou, W.; Yang, J.; Yang, J.; Huang, J.; Zhang, J.; Liu, Q.; Huang, S.; Bai, N.; Wu, Z.; Hong, W.; Wang, H.; Guo, C. F. Ionic Skin with Biomimetic Dielectric Layer Templated from Calathea Zebrine Leaf. *Adv. Funct. Mater.* **2018**, *28*, 1802343.
- (22) Wei, P.; Guo, X.; Qiu, X.; Yu, D. Flexible Capacitive Pressure Sensor with Sensitivity and Linear Measuring Range Enhanced Based on Porous Composite of Carbon Conductive Paste and Polydimethylsiloxane. *Nanotechnology* **2019**, *30*, 455501.
- (23) Highly Sensitive and Bendable Capacitive Pressure Sensor and Its Application to 1 V Operation Pressure-Sensitive Transistor. *Adv. Electron. Mater.* **2017**, *3*, 160045.
- (24) Ma, Z.; Wei, A.; Ma, J.; Shao, L.; Jiang, H.; Dong, D.; Ji, Z.; Wang, Q.; Kang, S. Lightweight, Compressible and Electrically Conductive Polyurethane Sponges Coated with Synergistic Multiwalled Carbon Nanotubes and Graphene for Piezoresistive Sensors. *Nanoscale*, **2018**, *10*, 7116.

- (25) Gong, S.; Schwab, W.; Wang, Y.; Chen, Y.; Tang, Y.; Si, J.; Shirinzadeh, B.; Cheng, W. A Wearable and Highly Sensitive Pressure Sensor with Ultrathin Gold Nanowires. *Nat. Commun.* **2014**, *5*, 3132.
- (26) Lou, Z.; Chen, S.; Wang, L.; Jiang, K.; Shen, G. An Ultra-Sensitive and Rapid Response Speed Graphene Pressure Sensors for Electronic Skin and Health Monitoring. *Nano Energy* **2016**, *23*, 7-14.
- (27) Zhu, B.; Niu, Z.; Wang, H.; Leow, W. R.; Wang, H.; Li, Y.; Zheng, L.; Wei, J.; Huo, F.; Chen, X. Microstructured Graphene Arrays for Highly Sensitive Flexible Tactile Sensors. *Small* **2014**, *10*, 3625-3631.
- (28) Chen, Z.; Wang, Z.; Li, X.; Lin, Y.; Luo, N.; Long, M.; Zhao, N.; Xu, J. B. Flexible Piezoelectric-Induced Pressure Sensors for Static Measurements Based on Nanowires/Graphene Heterostructures. *ACS Nano* **2017**, *11*, 4507-4513.
- (29) Lee, J.-H.; Yoon, H.-J.; Kim, T. Y.; Gupta, M. K.; Lee, J. H.; Seung, W.; Ryu, H.; Kim, S.-W. Micropatterned P (Vdf-Trfe) Film-Based Piezoelectric Nanogenerators for Highly Sensitive Self-Powered Pressure Sensors. *Adv. Funct. Mater.* **2015**, *25*, 3203-3209.
- (30) Mo, X.; Zhou, H.; Li, W.; Xu, Z.; Duan, J.; Huang, L.; Hu, B.; Zhou, J. Piezoelectrets for Wearable Energy Harvesters and Sensors. *Nano Energy* **2019**, *65*, 104033.
- (31) Ha, M.; Lim, S.; Cho, S.; Lee, Y.; Na, S.; Baig, C.; Ko, H. Skin-Inspired Hierarchical Polymer Architectures with Gradient Stiffness for Spacer-Free, Ultrathin, and Highly Sensitive Triboelectric Sensors. *ACS Nano* **2018**, *12*, 3964-3974.
- (32) Jeon, S. -B.; Kim, W. -G.; Park, S. -J.; Tcho, I. -W.; Jin, I. -K.; Han, J. -K.; Kim, D.; Choi, Y. -K. Self-Powered Wearable Touchpad Composed of All Commercial Fabrics Utilizing a Crossline Array of Triboelectric Generators. *Nano Energy* **2019**, *65*, 103994.

- (33) Lee, Y.; Cha, S. H.; Kim, Y. W.; Choi, D.; Sun, J. Y. Transparent and Attachable Ionic Communicators Based on Self-Cleanable Triboelectric Nanogenerators. *Nat. Commun.* **2018**, *9*, 1804.
- (34) Lin, Z.; Yang, J.; Li, X.; Wu, Y.; Wei, W.; Liu, J.; Chen, J.; Yang, J. Large-Scale and Washable Smart Textiles Based on Triboelectric Nanogenerator Arrays for Self-Powered Sleeping Monitoring. *Adv. Funct. Mater.* **2018**, *28*, 1704112.
- (35) Lin, Z.-H.; Cheng, G.; Yang, Y.; Zhou, Y. S.; Lee, S.; Wang, Z. L. Triboelectric Nanogenerator as an Active UV Photodetector. *Adv. Funct. Mater.* **2014**, *24*, 2810-2816.
- (36) Meng, X. S.; Wang, Z. L.; Zhu, G. Triboelectric-Potential-Regulated Charge Transport Through p-n Junctions for Area-Scalable Conversion of Mechanical Energy. *Adv. Mater.* **2016**, *28*, 668-676.
- (37) Rasel, M. S.; Maharjan, P.; Salauddin, M.; Rahman, M. T.; Cho, H. O.; Kim, J. W.; Park, J. Y. An Impedance Tunable and Highly Efficient Triboelectric Nanogenerator for Large-Scale, Ultra-Sensitive Pressure Sensing Applications. *Nano Energy* **2018**, *49*, 603-613.
- (38) Ren, Z.; Nie, J.; Shao, J.; Lai, Q.; Wang, L.; Chen, J.; Chen, X.; Wang, Z. L. Fully Elastic and Metal-Free Tactile Sensors for Detecting both Normal and Tangential Forces Based on Triboelectric Nanogenerators. *Adv. Funct. Mater.* **2018**, *28*, 1802989.
- (39) Shi, Q.; Zhang, Z.; Chen, T.; Lee, C. Minimalist and Multi-Functional Human Machine Interface (HMI) Using a Flexible Wearable Triboelectric Patch. *Nano Energy* **2019**, *62*, 355-366.
- (40) Xu, Z.; Wu, C.; Li, F.; Chen, W.; Guo, T.; Kim, T. W. Triboelectric Electronic-Skin Based on Graphene Quantum Dots for Application in Self-Powered, Smart, Artificial Fingers. *Nano Energy* **2018**, *49*, 274-282.

- (41) Yang, Y.; Zhou, Y. S.; Zhang, H.; Liu, Y.; Lee, S.; Wang, Z. L. A Single-Electrode Based Triboelectric Nanogenerator as Self-Powered Tracking System. *Adv. Mater.* **2013**, *25*, 6594-6601.
- (42) Wang, L.; Jackman, J. A.; Tan, E.; Park, J. H.; Potroz, M. G.; Hwang, E. T.; Cho, N. High-Performance, Flexible Electronic Skin Sensor Incorporating Natural Microcapsule Actuators. *Nano Energy* **2017**, *36*, 38–45.
- (43) Kim, K.; Hong, S.; Jang, N.; Ha, S.; Lee, H.; Kim, J. Wearable Resistive Pressure Sensor Based on Highly Flexible Carbon Composite Conductors with Irregular Surface Morphology. *ACS Appl. Mater. Interfaces* **2017**, *9*, 17499–17507.
- (44) Zhang, C.; Liu, S.; Huang, X.; Guo, W.; Li, Y.; Wu, H. A Stretchable Dual-Mode Sensor Array for Multifunctional Robotic Electronic Skin. *Nano Energy* **2019**, *62*, 164–170.
- (45) Park, J.; Lee, Y.; Hong, J.; Ha, M.; Jung, Y.; Lim, H.; Kim, S.; Ko, H. Giant Tunneling Piezoresistance of Composite Elastomers with Interlocked Microdome Arrays for Ultrasensitive and Multimodal Electronic Skins. *ACS Nano* **2014**, *8*, 4689–4697.
- (46) Huang, W.; Dai, K.; Zhai, Y.; Liu, H.; Zhan, P.; Gao, J.; Zheng, G.; Liu, C.; Shen, C. Flexible and Lightweight Pressure Sensor Based on Carbon Nanotube/Thermoplastic Polyurethane-Aligned Conductive Foam with Superior Compressibility and Stability. *ACS Appl. Mater. Interfaces* **2017**, *9*, 42266–42277.
- (47) Yang, Y.; Han, J.; Huang, J.; Sun, J.; Wang, Z. L.; Seo, S.; Sun, Q. Stretchable Energy-Harvesting Tactile Interactive Interface with Liquid-Metal-Nanoparticle-Based Electrodes. *Adv. Funct. Mater.* **2020**, 1909652.
- (48) Yao, G.; Xu, L.; Cheng, X.; Li, Y.; Huang, X.; Guo, W.; Liu, S.; Wang, Z. L.; Wu, H. Bioinspired Triboelectric Nanogenerators as Self-Powered Electronic Skin for Robotic Tactile Sensing. *Adv. Funct. Mater.* **2019**, 1907312.

- (49) Lee, Y.; Park, J.; Cho, S.; Shin, Y. E.; Lee, H.; Kim, J.; Myoung, J.; Cho, S.; Kang, S.; Baig, C.; Ko, H. Flexible Ferroelectric Sensors with Ultrahigh Pressure Sensitivity and Linear Response Over Exceptionally Broad Pressure Range. *ACS Nano* **2018**, *12*, 4045-4054.
- (50) He, J.; Xiao, P.; Lu, W.; Shi, J.; Zhang, L.; Liang, Y.; Pan, C.; Kuo, S.-W.; Chen, T. A Universal High Accuracy Wearable Pulse Monitoring System via High Sensitivity and Large Linearity Graphene Pressure Sensor. *Nano Energy* **2019**, *59*, 422-433.
- (51) Park, J.; Kim, M.; Lee, Y.; Lee, Y. S.; Ko, H. Fingertip Skin-Inspired Microstructured Ferroelectric Skins Discriminate Static/Dynamic Pressure and Temperature Stimuli. *Sci. Adv.* **2015**, *1*, e1500661.
- (52) Wang, Y.; Wang, Y.; Yang, Y. Graphene-Polymer Nanocomposite-Based Redox-Induced Electricity for Flexible Self-Powered Strain Sensors. *Adv. Energy Mater.* **2018**, 1800961.
- (53) Kim, M.; Choi, S.; Kim, H.; Han, S.; Moon, S.; Kim, E.; Kim, Y.; Park, K. Polymeric Redox Mediator as a Stable Cathode Catalyst for Lithium-O<sub>2</sub> Batteries. *J. Power Sources* **2020**, *453*, 227850.
- (54) Li, M.; Liu, T.; Bi, X.; Chen, Z.; Amine, K.; Zhong, C.; Lu, J. Cationic and Anionic Redox in Lithium-Ion Based Batteries. *Chem. Soc. Rev.* **2020**, *49*, 1688-1705.
- (55) Gao, L.; Zhu, C.; Li, L.; Zhang, C.; Liu, J.; Yu, H.; Huang, W. All Paper-Based Flexible and Wearable Piezoresistive Pressure Sensor. *ACS Appl. Mater. Interfaces* **2019**, *11*, 25034-25042.
- (56) Tsai, Y.; Wang, C. -M.; Chang, T. -S.; Sutradhar, S.; Chang, C. -W.; Chen, C. -Y.; Hsieh, C. -H.; Liao, W. -S. Multilayered Ag NP-PEDOT-Paper Composite Device for Human-Machine Interfacing. *ACS Appl. Mater. Interfaces* **2019**, *11*, 10380-10388.

- (57) Santos, A.; Pinela, N.; Alves, P.; Santos, R.; Fortunato, E.; Martins, R.; Águas, H.; Igreja, R. Piezoresistive E-Skin Sensors Produced with Laser Engraved Molds. *Adv. Electron. Mater.* **2018**, *4*, 1800182.
- (58) Liu, W.; Liu, N.; Yue, Y.; Rao, J.; Luo, C.; Zhang, H.; Yang, C.; Su, J.; Liu, Z.; Gao, Y. A Flexible and Highly Sensitive Pressure Sensor Based on Elastic Carbon Foam. *J. Mater. Chem. C* **2018**, *6*, 1451-1458.
- (59) Roh, E.; Lee, H. B.; Kim, D. I.; Lee, N. E. A Solution-Processable, Omnidirectionally Stretchable, and High-Pressure-Sensitive Piezoresistive Device. *Adv. Mater.* **2017**, *29*, 1703004.
- (60) Bae, G. Y.; Pak, S. W.; Kim, D.; Lee, G.; Kim, H.; Chung, Y.; Cho, K. Linearly and Highly Pressure-Sensitive Electronic Skin Based on a Bioinspired Hierarchical Structural Array. *Adv. Mater.* **2016**, *28*, 5300-5306.
- (61) Kohara, K.; Tabara, Y.; Oshiumi, A.; Miyawaki, Y.; Kobayashi, T.; Miki, T. Radial Augmentation Index: A Useful and Easily Obtainable Parameter for Vascular Aging. *Am. J. Hypertens.* **2005**, *18*, 11S-14S.

# Table of Contents

## Self-Powered Pressure Sensor

